J. Astrophys. Astr. (1989) **10,** 1–20

Optical Interferometric Observations of a Transient Event of 1986 March 13 in the Coma of Comet Halley

C. Debi Prasad, T. Chandrasekhar, J. N. Desai & N. M. Ashok
Physical Research Laboratory, Navrangpura, Ahmedabad 380009

Vinod Krishan *Indian Institute of Astrophysics, Bangalore 560034*

Received 1988 January 18; revised 1988 July 27; accepted 1988 November 25

Abstract. During the recent apparition of Comet Halley in 1985–86 a transient ionic event in the form of a blob of H_2O^+ emission was recorded in the coma at $\sim 0^h$ UT on 1986 March 13. Observations were carried out using a special IHW filter for H_2O^+ emission at 7000 Å/175 Å, a 35 cm telescope, a Fabry–Perot interferometer and an image intensifier camera from Gurushikhar, Mt Abu. (24°39′N, 72°47′E). A Fabry–Perot interferogram in Hα taken a few minutes later at the same location reveals strong hydrogen emission (Hα) associated with the blob. The velocity field in the blob is structured with relative velocities upto ~ 35 km s^{-1}. The event is interpreted as arising due to the sector boundary crossing of the interplanetary magnetic field by the comet.

Key words: Comet Halley- Hα Fabry–Perot interferometry—imaging—transient event

1. Introduction

During the perihelion passage of a comet, apart from the normal development of an extended coma, dust and ion tails, a number of less predictable events occur which provide clues about its composition and about the interaction of the cometary plasma with the solar wind. Dust jets originating from localized regions in the 'afternoon side' of the rotating nucleus produce non-gravitational accelerations or decelerations depending on the sense of rotation (Whipple 1950, 1951). Brightness flares of 1 to 2 magnitudes or more have been frequently reported in many comets like P/Schwassman-Wachmann 1, Morehouse 1908 III, Humason 1962 VIII (Wyckoff 1982), P/Tuttle–Giacobini–Kresak (Kresak 1974) and West 1975n (Cosmovici 1978). Suggestions have been made that outbursts in the cometary nuclei may be caused by chemical heating, by the presence of ices more volatile than H_2O^+ or by the exothermic crystallization of amorphous ice (Donn & Urey 1957; Whipple 1980). Comets during outbursts have shown enhanced CO^+ emission (Greenstein 1962; Festou *et al.* 1986) and it has been suggested that if a sudden phase change in H_2O ice is the outburst source then strong H_2O^+ emission might be observed (Wyckoff 1982).

The cometary ion tail exhibits a variety of dynamically active structures like streamers, kinks, helices and condensations resulting from the complex interaction of

the cometary plasma with the fast moving solar wind (Brandt 1982). At times dense clouds of plasma emanate from the coma, propagate down the tail and the sequence of events can be followed for several hours (Wolf 1909). The correlations of the ionization rate with solar wind behaviour (Jockers 1985) establishes the importance of ion exchange reactions between cometary neutrals and solar wind plasma. The dramatic tail disruptions or disconnection events (DE) have been extensively observed (Bobrovnikoff 1931; Jockers & Lust 1973; Jockers 1985; Burlaga *et al.*, 1973; Niedner & Brandt 1978, 1980; Ip 1980; Niedner IHW Newsletter No. 9 p. 2). The occurrence of DEs have been correlated with sector boundary of the interplanetary magnetic field crossing the comet tails and a mechanism for DEs has been suggested (Brandt 1968).

1.1 *Transient Events*

Apart from disconnection events which can be followed for several days, there have been reports of events even more transient. Barnard (1893) in his visual observations of the great comet of 1882 had noted transient features. Photographs of Comet Kohoutek taken on 19 January 1974 showed transient plasma features 10° away from the nucleus (Roosen & Brandt 1976). Transient features lasting ~ 1 hour have been reported at ~ 50 arcsec from the nucleus along the sun-comet line of Giacobini–Zinner on several occasions (Telesco *et al.* 1986). The spectrophotometric observations of Comet IRAS–Araki–Alcock 1983d between 4000 Å and 4900 Å obtained on the night of 1983 May 9/10 revealed an abrupt and dramatic brightening of the inner coma during a 20 minutes interval, preceded and followed by periods of normal stability (Lutz & Wagner 1986). Several possible mechanisms such as the outburst of ices from the nucleus and a compression wave in the solar wind enhancing the gas and dust density of the coma were invoked to explain these observations. Russell & Luhman (1987) have pointed out that due to the alignment of the interplanetary magnetic field with the solar wind flow, the coma could not have been shielded from the solar wind as a result of weak mass loading. This could have given rise to a Venus-like interaction (Alexander, Luhman & Russell 1986) producing large ionization deep inside the coma.

In its recent apparition, Comet Halley has also exhibited some transient features. Elongated jet-like structures moving rapidly have been seen on blue and red images during 1985 November (Grun *et al.* 1986; Jockers 1985). These observations show a large, curved, jet-like structure extending 21 arcmin to the south of the cometary nucleus nearly perpendicular to the projected antisolar direction. An image taken ~ 3.5 hours later shows that the direction of strongest emission had shifted by 10°. Study of the Giotto observations and the corresponding ground-based observations have also revealed short-lived plasma phenomena lasting less than an hour.

In this paper we present observations of a transient event in the coma of Comet Halley in the form of a strong H_2O^+ emission blob at $\sim 2 \times 10^5$ km from the nucleus, and an Hα interferogram from an extended region surrounding the blob (Chandrasekhar *et al.* 1987). The paper discusses the observational details, the interferogram analysis and outlines a possible cause for the occurrence.

2. Methods of observation and analysis

2.1 *Instrumentation*

A 35-cm aperture f/11 telescope with an imaging Fabry-Perot (FP) spectrometer was used for observations of Comet Halley at Gurushikhar (24°39′N, 72°47′E, 1700 m altitude), Mt Abu, India. Fig. 1 gives a schematic layout of the instrument. The image formed at the focal plane of the telescope A, collimated by lens L was passed through the Fabry–Perot etalon E and narrowband filter F before being reimaged on the photocathode of the light image intensifier (I) by the camera lens O. The interferogram formed on the photocathode was recorded on Kodak 2415 emulsion held in proximity with the phosphor screen. The instrument was also used as an imaging device to produce broadband filter imageries in the IHW filters of the cometary coma (Chandrasekhar *et al.* 1988). Parameters related to instrumentation are listed in Table 1.

Spectral calibration with a He–Ne laser or a low-pressure Mercury spectral lamp was taken every night to define the instrumental profile. Step-wedge intensity calibration was impressed on the film every night to enable relative intensities to be deduced from measured photographic densities.

The observational period of 8 months from 1985 October to 1986 May covered a wide range of heliocentric distance of the comet. The data reported here concern, in particular, the interferogram and the images taken on 1986 March 13. Table 2 gives the parameters of Comet Halley during these observations.

2.2 *Observations*

Table 3 gives the journal of the observations on 1986 March 13. While selecting frames for digitization it was noticed that the frames on that day show additional features and that Hα interferogram had also been recorded on the same day (Fig. 2). Fig. 2a is the white light frame wherein a projection in one direction is readily seen. Figs 2b and c are H_2O^+ jmageries of the coma taken ~40 minutes after the white light frame and distinctly feature the blob. The blob is at a projected distance of 2×10^5 km from the nucleus and occupies an extent 30000 km × 20000 km in the plane of the sky. The blob is seen at a position angle 160° measured North through East relative to the nucleus. In the interferogram frame at least three fringes are clearly

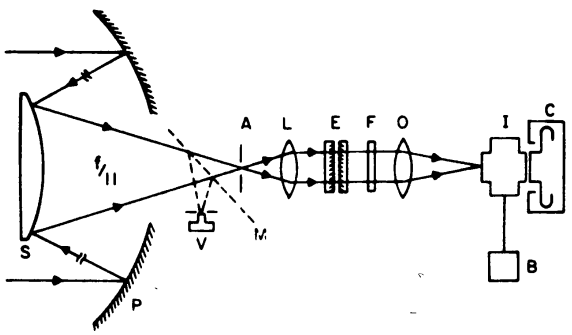

Figure 1. Schematic diagram of the interferometer optics.

Table 1. Parameters of instrumentation.

1. *Etalon parameters*		
Spectral coverage		5700–6700 Å
Spacer value		1000 μm
Usable aperture		24 mm
Plate flatness		$\lambda/100$
Free spectral range		2.15 Å
Effective finesse		~ 20
Effective instrumental width		~ 0.11 Å
2. *Image intensifier*		
Effective diameter of multialkali photocathode		25 mm
Spectral range		3500 Å to 9100 Å
Limiting spatial resolution at centre at 5 per cent MTF level		30 line pairs mm^{-1}
Maximum image distortion near edge compared to centre		5 per cent
Magnification		1.2
Image scale size on the camera		67 arcsec mm^{-1}
Field of view on the sky		21 arcmin
3. *Interference filters*		
Peak wavelength λ(Å)	FWHM $\Delta\lambda$(Å)	Peak transmission per cent
6563 (Hα)	5	40
7000 (H_2O^+)	175	80

Table 2. Parameters of Comet Halley during observations.

Date	AU Δ	km s^{-1} $\dot{\Delta}$	AU r	km s^{-1} $\dot{r}$	V(orbital) km s^{-1}	Parker's spiral angle
March 13 0^h UT	0.98	−43.18	0.89	25.47	45	42°

seen. In the microdensitometric tracing fainter fringes and structures in the fringe profile can be recognized. The blob feature was shown to be definitely associated with the comet after a careful consideration of various possibilities which are detailed in Appedix I.

The details of digitization of the Hα interferogram, H_2O^+ and white light pictures, and processing of the digitized images are given in Appendix II. Fig. 2d shows the interferogram in Hα taken with a 5 Å bandwidth filter with an exposure of 11 minutes.

2.3 *Fringe-Shift Analysis*

Careful microdensitometric measurements of the fringe diameter have been made and the instrumental parameters precisely defined using He–Ne laser interferogram. A

Table 3. Journal of observations.

S. No.	UT of exposure	Exposure	Filter
1	March 12 23:26:55	1^s	white light
2	March 12 23:29:30	5^s + Laser (flash)	white light + laser
3	March 13 00:06:34 00:09:34	3m	7000 Å/175 Å H_2O^+ filter
4	March 13 00:10:17 00:15:17	5m	7000 Å/175 Å H_2O^+ filter
5	March 13 00:18:54 00:30:00	$11^m\,06^s$	6563/5 Å Hα interferogram

careful comparison was made with an earlier Hα interferogram on the Orion trapezium region, which served as a celestial spectral reference of known radial velocity relative to the earth. From the measurements of the fringe shift, we obtain for the blob a recession radial velocity of 30 ± 10 km s^{-1} relative to the comet (as seen from the earth). The interfringe separation and hence the relative velocity distribution can be better determined than the net absolute radial velocity. A procedure for determining the relative velocity distribution is detailed in Appendix III. The relative velocity values are given in Table 4 and their spatial distribution is featured in Fig. 3.

In addition to the determination of the velocity structure in the blob line-profile analysis of a few bright portions of the Hα interferogram has also been carried out in order to study the local dynamics of the hydrogen gas in the blob. Fig. 4 shows some line profiles which can be seen to be asymmetric, indicating non-isotropic flow of gas in the blob. The profiles close to the blob centre are highly structured. Least-square Gaussian profiles were fitted to the data to obtain the equivalent widths and hence internal expansion velocities. Table 5 summarizes the internal velocities obtained from the line profile analysis. There is evidence for fringe splitting at several places in the interferogram, which unambiguously establishes the existence of large differential velocities in the blob.

3. Discussion

The differential velocity field derived from the Hα interferogram and the line-profile measurements show a complex structure. The exact mechanism of the event is not quite clear at present. However, here we discuss the broad characteristics of the data and their implications to the understanding of the transient events in the cometary atmosphere.

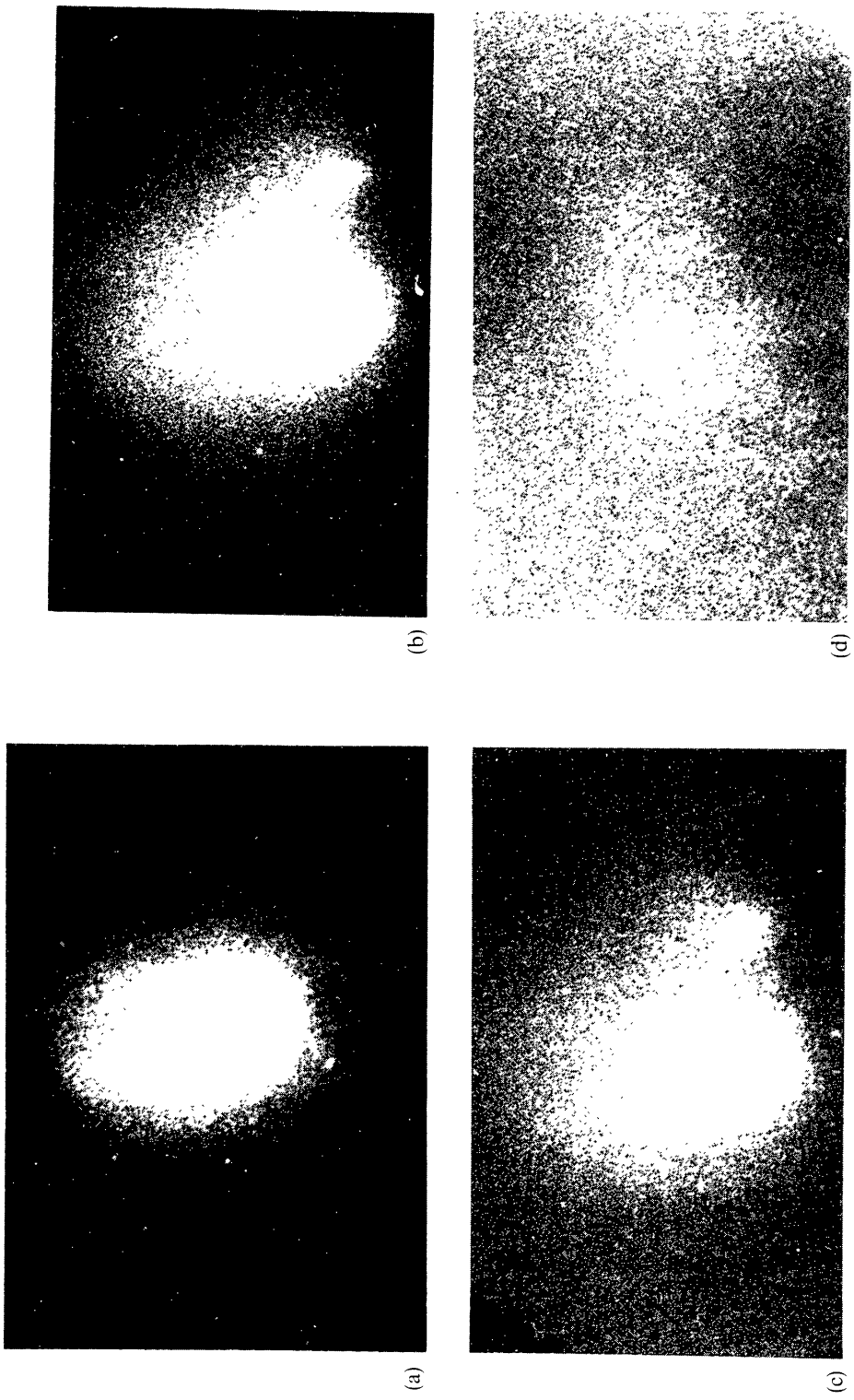

Figure 2. (a) White light frame taken at 1986 March 12: $23^h\ 26^m\ 55^s$ (1^s exposure). (b) H_2O^+ frame (3^m exposure) at 1986 March 13: $00^h\ 08^m\ 04^s$ (mean). (c) H_2O^+ frame (5^m exposure) at 1986 March 13: $00^h\ 12^m\ 47^s$ (mean). (d) Hα frame (6563/5 Å)-11^m exposure taken at 1986 March 13: $00^h\ 24^m\ 27^s$ (mean).

Table 4. Relative radial velocity determination from line shifts.

S. No.	Position angle in degrees	Distance 10^4 km	Internal velocity km s^{-1}
1	203	31.3	20 ± 2
2	200	28.7	23 ± 2
3	192	23.3	9 ± 2
4	187	36.7	10 ± 9
5	185	30.7	23 ± 6
6	181	24.7	-1 ± 2
7	178	38	5 ± 10
8	178	36.7	21 ± 8
9	178	34	-21 ± 8
10	178	31.3	-27 ± 6
11	178	24.7	0.0
12	175	24.7	11 ± 1
13	174	31.3	-4 ± 2
14*	171	33.3	-15 ± 2; -36 ± 2
15	171	23.3	2 ± 5
16	170	23.3	1 ± 3
17	168	30	18 ± 8
18	167	32.7	1 ± 10
19	166	22.7	4 ± 2
20	166	33.3	1 ± 10
21	165	30	-6 ± 8
22	164	33.3	26 ± 11
23	163	22	9 ± 2
24	163	29.3	5 ± 3
25	160	32	37 ± 6
26	160	20.7	-6 ± 1
27	160	14	4 ± 1
28	158	15.3	-18 ± 1
29	158	16.7	-16 ± 1
30	158	17.3	5 ± 1
31*	158	18.4	11 ± 1; 1 ± 1
32	158	19.7	16 ± 1
33*	157	28	2 ± 1; -25 ± 1
34	154	30.7	-43 ± 9
35	153	26.7	-9 ± 6
36	150	25.3	1 ± 2
37	148	28.7	4 ± 8
38	145	27.3	10 ± 2
39*	145	24	32 ± 1; 19 ± 2
40	145	30.8	15 ± 9
41	145	32.7	1.1 ± 10
42	144	29.3	0 ± 2
43	143	22.7	21 ± 2
44	142	28	6 ± 2
45*	140	20.7	5 ± 1; -3 ± 2
46*	137	18.7	32 ± 1; -10 ± 2
47	135	22.3	1 ± 2
48	135	16.7	-9 ± 2
49	135	15.3	18 ± 2
50*	133	12.7	12 ± 2; 33 ± 2
51	138	18	8 ± 2
52	135	16	27 ± 2

* Split fringe.

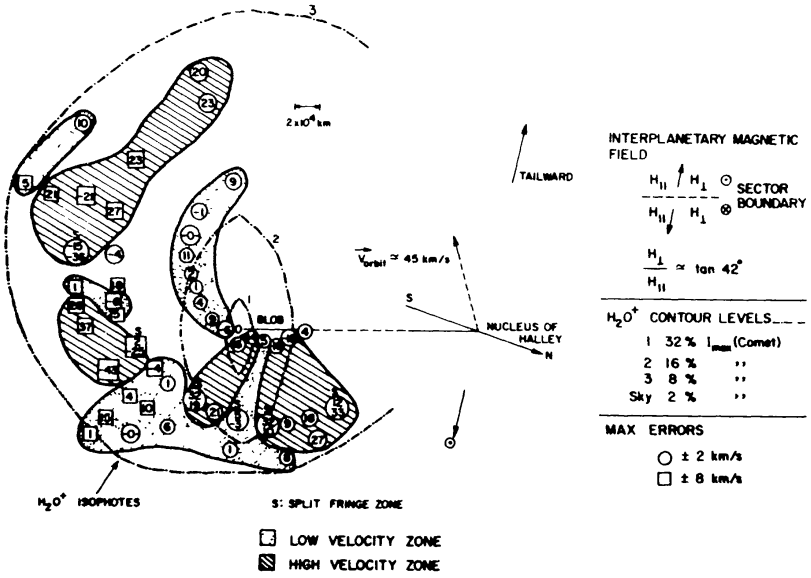

Figure 3. Doppler-shift dispersion velocity distribution in the H_2O^+ blob region. H_2O^+ isophote contour levels are drawn approximately from Fig. 7(a).

3.1 *State of the Coma Activity on 1986 March 13 from Other Observations*

As the event took place only 24 hours before the Giotto encounter with Halley the cometary coma was under close observation. Unfortunately Giotto cameras were not on at the time of the event to provide confirmation of our event. The white light images taken at South African Astrophysical Observatory at $2^h\ 32^m\ 05^s$ UT (~ 2.5 hours after our observations) do not show a blob. Three different jet-like structures at 65.5°, 87.5° and 102.5° (angle with respect to sun) appearing in the E–S direction, confined to the inner coma region 20000 to 35000 km from the nucleus are however seen. A comparison of red filter pictures of 1986 March 13 and 14 shows that the dust activity was more on March 13 compared to March 14 by a factor of ~ 2 (Cosmovici *et al.* 1986). Evidence of such activity is also observable in the images taken at 0415 UT on March 13 at Catania observatory in Italy (Formisano *et al.* 1986). Dust concentration in the vicinity of the nucleus was also monitored at the 3.9-m Anglo-Australian telescope on 1986 March 11, 12 and 13. Development of the jets over a period of 3 days could be traced in the photographs but again there is no evidence for a blob structure (Chakaveh, Green & Ridley 1986).

The Lyα images taken at $10^h\ 54^m$ UT on March 13 do not show any asymmetry beyond $\sim 10^5$ km from the nucleus indicating the hydrogen gas flow to be unaffected by the cometary activity (McCoy, Opal & Carruthers 1986). Photometric observations during the period 1986 March 5–17 show a day-to-day variation of intensities in several emission bands. The data show an enhancement by a factor of about two in the production rate of all observed species on March 13 compared to the neighbouring days but there are several days during the observational period when such enhancements occurred. (Schleicher *et al.* 1986).

Festou *et al.* (1986) have reported an enhanced count rate in IUE fine error sensor in 12×12 arcsec aperture at 19^h UT on March 13 indicating an increase in the

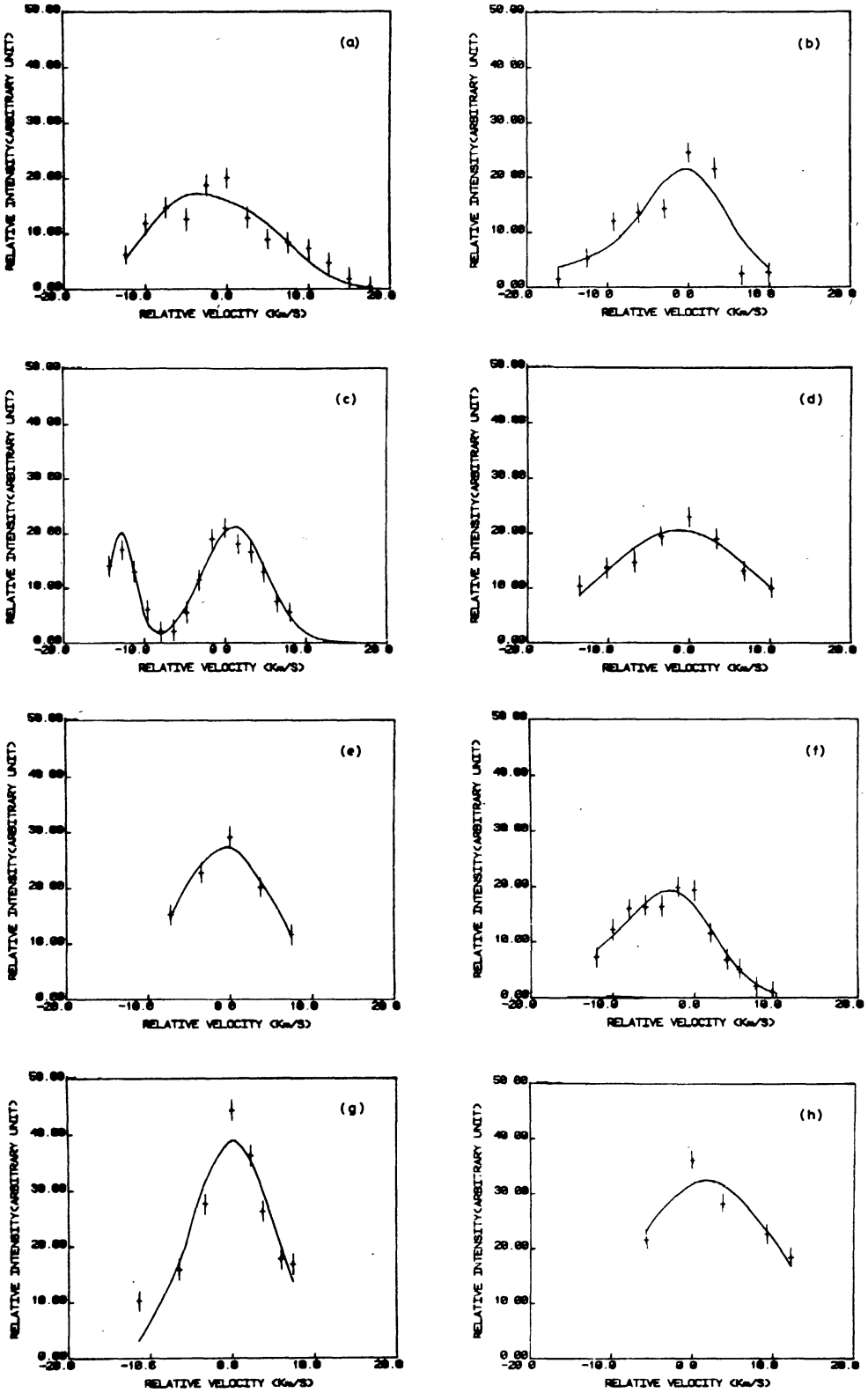

Figure 4. Line profiles from selected regions of the interferogram at (a) PA: 174, d: 24.7; (b) PA: 140, d: 20.7; (c) PA: 160, d: 17.3; (d) PA: 135, d: 22.7; (e) PA: 127, d: 18.0; (f) PA: 180, d: 23.3; (g) PA: 200, d: 28.7; (h) PA: 204, d: 30.7; where PA = position angle, and d = cometocentric distance in 10^4 km.

Table 5. Doppler line-width velocity from line profiles.

S. No.	Position angle in degrees	Distance 10^4 km	Internal velocity km s^{-1}	Comments
1	174	24.7	11 10	split $\sim$ 7.5 km s^{-1}
2	140	20.7	10 6	split $\sim$ 6.6 km s^{-1}
3	160	17.3	8 <5	split $\sim$ 12.8 km s^{-1}
4	135	22.7	22	
5	127	18.0	13	
6	180	23.3	10 16	
7	200	28.7	10	
8	204	30.7	21	

cometary visual brightness. The spectra indicate enhanced H_2O and CS production rates. Observations with spectral resolution at the wavelength of Hα have been carried out by Kerr *et al.* (1987) from Arecibo observatory. Observations in 1986 March are characterized by highly structured Hα profiles implying nonisotropic outflow of H atoms. Velocities relative to the comet of 35 km s^{-1} have been noted from the position of the fringe peaks. The observations for March 13 give a Hα surface brightness of 59 ± 13 Rayleighs for a 5.9 arcmin field of view. The profile analysis show that Hα emission was confined to highly directional flow indicating the association of jet activities. From the observations discussed above we are led to the conclusion that while 1986 March 13 was a day of enhanced dust activity it was not an unusual one. The absence of the blob at other longitudes suggests that the ionic event observed by us is a transient one lasting a few hours only and that the cause is likely to be external to the comet. The few images of the comet reported over Indian longitudes on this day are on a scale too coarse for the blob to be discerned (A. Desai *et al.* 1987; A. K. Bhatnagar 1987, personal communications).

However, there appears to be some evidence for transient ionic features lasting $\sim$1 hour in the inner coma of Comet Halley. Ip, Cosmovici & Mack (1986) have inferred such an event by comparing the ground-based SAAO CCD H_2O^+ observations with the Giotto NMSE and IMSE measurements of Comet Halley. These instruments on Giotto had recorded a plasma pile up region at $\sim 10^4$ km from the nucleus which should have showed up in the ground-based CCD images as inhomogeneous structures. It is also the inference of Ip, Cosmovici & Mack (1986) that the clear absence of such structures in the CCD images suggests their rapid time variability $\sim$1 hour. Blobs in the Comet Halley were also detected in OH radio observations by de Pater *et al.* (1986).

In the case of Vega-1 encounter, the SDA sensor observed a burst of ions with energies $\sim$100–1000 eV near the closest approach to Comet Halley lasting $\sim$5 minutes. Based on the magnetic field observations in the path of the spacecraft

(Verigin *et al.* 1987) concluded that the burst was produced by the motion of cometary ions of water-group accelerated upto superalfvenic speeds. Further they point out that the acceleration could be caused by merging of interplanetary magnetic field lines of opposite polarity retarded by the presence of cometary plasma and neutrals. Such observations of well-defined intensity enhancement of ions >40 keV are reported from Tunde-M experiment on board Vega-1 (Somogyi *et al.* 1986).

The theoretical studies have shown several possible explanations for such light outbursts in the cometary ionosphere (Delsemme 1979). The rapid ionization of the gaseous material in the coma can be achieved by the discharge of cross-tail electric current. Such ionization surge, well within the coma, can also be caused by electron jetting in the reconnection current sheet which is produced by the passage of an interplanetary sector boundary through the comet (Niedner 1980).

3.2 *State of the Interplanetary Magnetic Field*

Since it is conjectured that the event seen could be a special type of disconnection event caused by the passage of an interplanetary magnetic field boundary through the comet it is pertinent to enquire about the state of the interplanetary magnetic field at the time of the event.

Comet Halley was predicted to enter a current sheet warp at about the time of the Japanese cometary space probe Sakigake's encounter on 1986 March 11, and to exit from it two days later (Niedner 1986). Based on the diagram of Carrington rotation 1772 Niedner & Schwingenschuh (1986) have discussed the interplanetary sector boundary configuration on these days. The observations from Sakigake and Giotto show that it was indeed the case (Saito *et al.* 1986; Neubauer *et al.* 1986). The multiple crossing of the current sheet by the comet during 1986 March 11–14 was clearly evident from Sakegake's measurements, which located the sector boundary at 7×10^6 km upstream of Comet Halley. It is known that only if the comet penetrates the sector boundary perpendicularly can major ionic tail disconnection events take place (Niedner & Brandt 1978). However, since no major DE was observed during this period, Saito *et al.* (1986) proposed that the crossing of the sector boundary by the comet was quasi-parallel. The Sun–Comet–Earth geometry and the Parker's spiral at the time of our observation is given in Fig 5. Since the comet was crossing the ecliptic plane at this time, sun, comet and earth can be considered to be in the same plane. According to Saito *et al.* (1986) the comet crossed the neutral sheet at a small attack angle. Considering the motion of the comet, they pointed out that, the southern part of Halley dipped first into the away sector, changing the polarity of the field line from towards to away polarity. Though the authors argue that the gradual reconnections of field lines may not lead to a drastic DE, no quantitative picture is outlined.

Further, if the radial alignment of the field occurred at that time the inner region of the coma could not have been shielded from the solar wind flux, which could have led to an enhanced ionization as in the case of Venus and Comet IRAS–Araki–Alcock (Russell & Luhmann 1987). The timescale of ionization by these processes are found to be very short $\sim 10^3$–10^4 s.

The geometry of the reconnecting magnetic fields is qualitatively represented in Fig. 6. Here, the magnetic field lines of reversed polarity flow towards each other at a relative velocity in the Z-direction, are cut in the diffusion region (the hatched area)

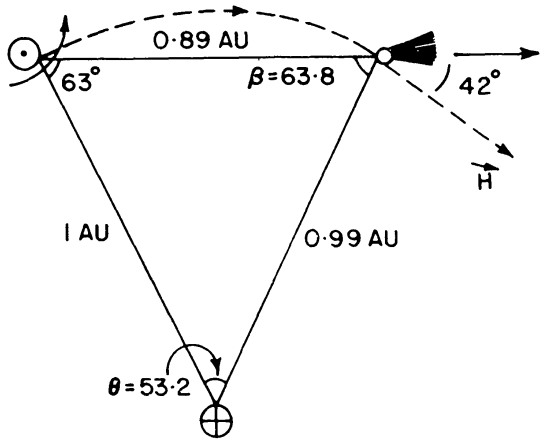

Figure 5. Sun–Comet–Earth geometry and the interplanetary magnetic field structure during observations.

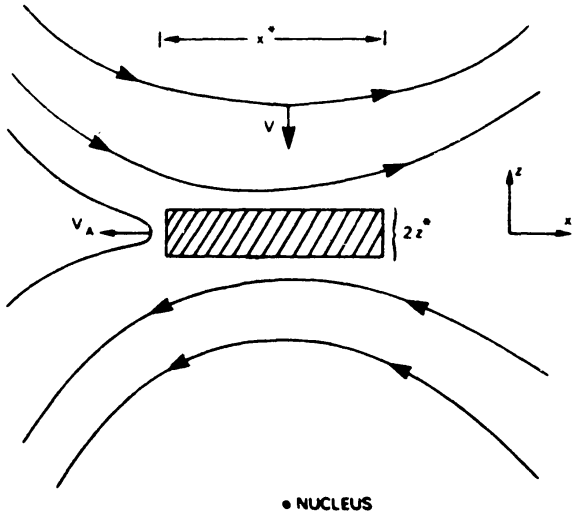

Figure 6. Geometry of reconnecting magnetic fields just before a disconnection event (DE); the direction of plasma outflow from the diffusion region (shaded) is given by $\mathbf{V}_A$.

and the reconnected field lines flow out of the diffusion region in $\pm x$-direction. The $\mathbf{v} \times \mathbf{B}$ driven electron jets in the reconnection current sheet would then produce sufficient energy to create a rapid ionization region.

3.3 *Kinematics of the Blob*

The relative radial velocity measurements show a complicated velocity field as represented in Fig. 3. However, dividing the map into high and low velocity zones, it can be noticed that the velocities are clustered into compact regions. There are some zones of high relative velocity. A number of split fringes are also seen especially on the Sunward side. The velocity distribution around the blob is also not symmetrical, indicating thereby that the expansion of the blob is not simply governed by the diffusion process.

Estimate of time of dispersal

Assuming the surface brightness of a spherical blob to vary as $1/r^2$ and an isotropic constant expansion velocity of 30 km s^{-1} it is possible to estimate crudely the time taken (τ) by the blob intensity (I_0) to reach the background sky level (I). The time of dispersal of the blob is given by

$$\tau \simeq \frac{R_0}{V}\sqrt{I_0/1}.$$

For $I_0/1 \sim 8.1$, $2R_0 \sim 3 \times 10^4$ km, and $V \sim 30$ km s^{-1}, $\tau \sim 23$ minutes.

A slowing down of the dispersal velocity would result in a longer period of visibility. However, it is unlikely that the blob will survive for more than a few hours. The short life span can explain the lack of sightings of the blob by groups located at other longitudes.

Mass

Assuming the blob to be spherically symmetric to a first approximation, with a $2 \times 10^{22}/r^2$ (cm) dependence of H_2O^+ number density we estimate the mass of the blob to be

$$\int_{\text{Extent of the blob}} 4\pi n(H_2O^+) r^2 \, dr \simeq 10^{10} \text{ g}.$$

Most of the line profiles are structured. A few of them are good enough to be considered for Gaussian analysis. The line profile analysis indicates the relative velocity spread of 5 to 22 km s^{-1} in reasonable agreement with the Doppler shift velocities measured in the blob (Fig. 4).

4. A theoretical model for the event

Based on the knowledge that a sector boundary crossing had taken place during the time of the event, a theoretical model for the formation and movement of the blob is suggested below.

The plasma tail disconnection events in Comets are believed to be caused by magnetic reconnection which occurs due to the passage of a sector boundary through the cometary head (Niedner & Brandt 1978, 1979, 1980). One of the consequences of the magnetic reconnection is that plasma flows out of both sides of the reconnection region at the Alfven speed as shown in Fig. 6. We propose that the ejection of H_2O^+ blob observed by us on March 13 is caused by magnetic reconnection. The blob during its outflow in the solar wind is constrained by the pressure balance equation

$$\frac{B_c^2}{4\pi}\left(\frac{R_0}{R_s}\right)^2 + \rho_c\left(\frac{R_0}{R_s}\right)^2 V_c^2 = \rho_s V_s^2 \qquad (1)$$

where ρ_c is the blob density at R_0 and is assumed to vary as r^{-2}; B_c is the magnetic field at R_0 and is assumed to vary as r^{-1}; V_c is the outflow velocity which is close to

Alfven velocity V_A in the Cometary head and is assumed to remain constant; R_0 is the initial position of the blob, measured from the nucleus. ρ_s and V_s are the density and velocity of solar wind and R_s is the observed separation of the blob from the comet head in the H_2O^+ frames. Magnetic field of the solar wind is taken to be much smaller than the cometary magnetic field and is neglected.

From Equation (1) one finds

$$\left(\frac{R_s}{R_0}\right)^2 = \frac{2V_A^2\rho_c}{V_s^2\rho_s}. \tag{2}$$

The time τ taken for the blob to reach R_s is given by

$$\tau = \frac{R_s - R_0}{V_A}. \tag{3}$$

From the measurements made by Vega space missions to Comet Halley it follows that the number density of H_2O^+ ions at a distance of $\sim 10^4$ km from the nucleus has a value $\sim 3 \times 10^3\,\mathrm{cm}^{-3}$ and varies approximately as $1/R^2$ where R is the distance to the comet's nucleus. The plasma convective velocity estimates imply a velocity $2-3$ $\mathrm{km\,s}^{-1}$ at $\sim 10^4$ km which rises to $\sim 20\,\mathrm{km\,s}^{-1}$ at $\sim 2 \times 10^5$ km, the distance from the nucleus at which the H_2O^+ blob is seen (R_s) (Vaisberg *et al.* 1987). Putting in the values $V_A \sim V_c \sim 20\,\mathrm{km\,s}^{-1}$, $V_s \sim 450\,\mathrm{km\,s}^{-1}$, $\rho_s \sim 1.7 \times 10^{-25}\,\mathrm{g\,cm}^{-3}$ (10 solarwind protons cm^{-3}), $\rho_c \sim 10^{-19}\,\mathrm{g\,cm}^{-3}$, we get $R_0/R_s = \left(\frac{\rho_s}{2\rho_c}\right)^{1/2}\frac{V_s}{V_A} \sim \frac{1}{5}$. Therefore the initial position of the blob should be 4×10^4 km from the nucleus. The time taken by the blob to reach the position $R_s \sim 2 \times 10^5$ km is given by

$$\tau = \frac{R_s - R_0}{V_A} \sim 2.2 \text{ hours}.$$

The cometary magnetic field at the initial position R_0 is

$$\sqrt{4\pi\rho_c}\,V_A \sim 200\gamma \quad \text{and} \quad \text{at } R_s \text{ is } \sim 10\gamma.$$

Giotto measured a magnetic field of $\sim 60\gamma$ much after this event took place. However, the cometary magnetic field B_c may appear to be rather high but is not unacceptable especially when the field is expected to undergo compression in the cometary head. *Thus plasma outflow caused by magnetic reconnection provides a reasonable description of the* H_2O^+ *blob.*

5. Summary and conclusion

Fabry–Perot interferometric observations along with the H_2O^+ emission imagery data taken at $\sim 0^h$ UT on 1986 March 13 reveal a transient ionic activity in the coma of Comet Halley.

1) A distinct extended brightness region (blob) in the H_2O^+ image is clearly seen at position angle 160° relative to the nucleus at 2×10^5 km projected distance in the plane of sky.

2) An Hα interferogram is recorded in the region of H_2O^+ blob. Interferogram analysis shows:

(i) The blob has a recession radial velocity of $\sim 30 \pm 10\,\mathrm{km\,s^{-1}}$ relative to the comet (as seen from the earth).

(ii) Gaussian analysis of the line yields Doppler line-width velocities from 5 to $22\,\mathrm{km\,s^{-1}}$.

(iii) The relative differential velocity map exhibits a structured distribution. High velocity and low velocity regions are clustered. Fringe splitting is observed at many places on the Sunward side.

(iv) The dispersal time at the blob is estimated to be approximately ~ 30 minutes. The event is definitely a transient one.

3) An upper limit to mass of the blob should be $\sim 10^{10}$ g.

4) The comet was crossing interplanetary sector boundary at about the time of observations. An explanation of the event is attempted from the state of the interplanetary magnetic field geometry in the vicinity of the comet. Our event appears at a time when disconnection events are most expected. However, it occurs in a region of the coma and not in the ionic tail wherein are triggered the normal disconnection events. The direction of the blob movement and its duration are unlike a typical disconnection event. The ejection of the blob in a direction not along the tail is a consequence and a test of the magnetic reconnection occurring in the head of the comet.

In conclusion, we would like to stress on the need for close monitoring of a comet, particularly in the ionic emissions like H_2O^+ or CO^+ during its period of maximum activity to ensure that the transient events like the one reported here are not missed out. Such events by many observers can provide valuable insights into this intriguing aspect of cometary behaviour and the interrelationship with the interplanetary medium.

6. Acknowledgements

This work was financially supported by the Department of Space, Government of India. The digitization of the photographic frames was carried out at the PDS facility of the Indian Institute of Astrophysics, Bangalore. The contour maps were made at the National Image Processing Facility in Astronomy, Ooty. Mr H. I. Pandya's computational assistance is gratefully acknowledged. The authors would also like to thank Dr David Rees of the University College, London for useful discussion on the particular event. Finally the comments of the unknown referee towards improving this paper are also gratefully acknowledged.

Appendix I
Association of the blob with the comet

The emergence of the blob and its association with the comet is verified from the following facts:

(1) An extensive search of star catalogues by us and by Dr David Rees of University College, London (Personal communication, 1987) showed that no star brighter than

11th magnitude existed near the feature. The feature is definitely brighter than this limit and is not a compact object.

(2) Search for a nebular object in the vicinity of the blob in the NGC catalogue of nonstellar objects (Sulentic & Tifft 1973) also led to a negative result, thereby ruling out nonstellar astronomical objects down to the magnitude 16.

(3) That the feature is not an instrumental artefact due to a possible reflection in the filters is confirmed by repeated checks of the instrument.

(4) Out of about 200 photographs taken with similar filters, only on this occasion is such a blob feature noticed.

(5) The region of enhanced brightness in H_2O^+ correlates with a feature in the white light frame where no filter was used.

(6) The Hα interferogram is obtained in the same region of the blob. It is recorded only on this day implying an interconnection with the event. Our instrumental sensitivity does not permit the recording of the geocoronal Hα. On this basis certain upper limits of the observed Hα emission can be deduced ($\lesssim 60\,R$).

Appendix II
Digitization and image analysis

The H_2O^+ images and the Hα interferogram recorded on photographic films were digitized with a 1010M (Perkin–Elmer) PDS microdensitometer system. The digital images have a pixel size of 20 μm which is comparable with the intensifier resolution to produce the continuous tone image of the film. The gray level in each pixel is represented by 8 bit binary numbers and stored in a standard format (Pub No: TM 16913250, Perkin–Elmer corporation). Each horizontal scan of the image is stored as

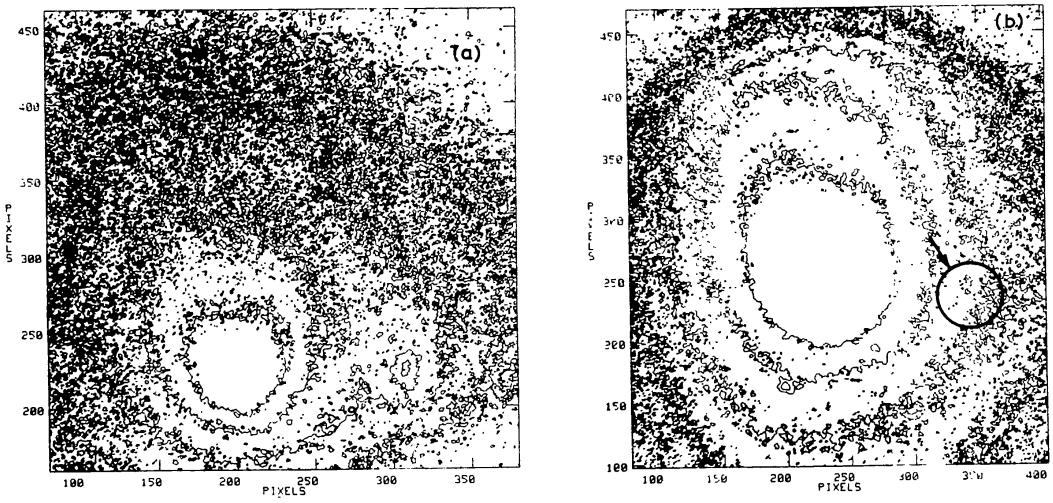

Figure 7. (a) Isophotes for H_2O^+ image of Comet Halley at 1986 March 13: $00^h\,12^m\,47^s$ (5 m exposure). Contour levels are at 4, 8, 12, 32 per cent of the peak photographic density. (b) Isophotes for white light image of Comet Halley of 1986 March 12: $23^h\,26^m\,55^s$ (1 s exposure). Contour levels are at 4, 8, 16, 32 per cent of the peak photographic density. The contour asymmetry corresponding to the position of the H_2O^+ blob in Fig. 3 is shown with a circle marked by an arrow.

one record of the image file. An image file contains about 1000 such records corresponding to the number of horizontal scans required to complete the image. The digital images were computer processed to enhance the faint features. In order to obtain the sharp intensity gradients the local background was removed from the digital image. The median-filter algorithm with a 10×10 pixel window was used to generate a lowpass 'model' of the image, representing all the largest structural information in the image. This low-pass model was then subtracted from the unprocessed image to produce a high-pass filtered picture. Fig. 7(a) shows the isodensity contours of the H_2O^+ image. A distinct blob is clearly seen at position angle 160° (measured from north through east) with respect to the nucleus. The blob is at a projected distance of 2×10^5 km in the plane of the sky from the nucleus. The isodensity contours of the white light image in Fig. 7(b) also show a distinctive projection (in terms of contour asymmetry) in the same region as the blob in the H_2O^+ frame. The contrast-enhanced image shows that the extent of the blob in the plane of the sky is 30000 km × 20000 km and the peak brightness ratio of the blob to the comet nucleus is < 0.12.

Appendix III
Radial scan analysis and determination of differential velocity map

In order to obtain the relative velocities of different parts of the H_2O^+ blob, a number of radial scans were taken from the centre of the interferogram and fringe shifts were measured. It is first necessary to very precisely locate the fringe centre.

Determination of Interferogram Fringe Centre

The digital interferogram was displayed on the image monitor and the approximate position of the fringe centre was determined by a visual inspection. Its precise location was then obtained by using a task 'IRING' of the Astronomical Image Processing System (AIPS) environment. In this task the approximate centre obtained by visual inspection, and the diameter and width of the second ring are given as inputs to obtain the integrated gray value of the annulli. The procedure was repeated shifting the position of the centre to its neighbouring pixels. The pixel giving the maximum value of integrated flux of annular ring was taken as the pixel defining the centre of the FP fringe system. With this procedure the fringe centre could be determined to an accuracy of two pixels ($\sim 40\,\mu$m on the film).

Retrieval of the Radial Scan

The interferogram was sampled along radial directions at various angles with respect to the horizontal references scan. The record number (Y-coordinate) containing the centre of the interferogram can be directly used as one radial scan of the interferogram. Since the pixel sizes of the digital interferogram image is 20 μm the sampling error in this case is also 20 μm. However, while obtaining the radial scan along other directions the sampling error depends on the angle of the scan direction with respect

to the horizontal scan. In this case the record numbers were incremented or decremented with respect to the record number of the horizontal scan and the corresponding position of the data point was calculated by specifying the desired angle. The sampling error is given by (for non zero values of θ)

$$\Delta X' = \frac{\Delta X}{\sin\theta}. \tag{1}$$

Where, $\Delta X = 20\,\mu$m and $\Delta X'$ is the sampling step in the direction defined by θ.

Velocity Determination

To obtain the wavelength corresponding to the observed radius of the fringe in the interferogram a search grid was generated to obtain a number of sets of possible radii values within the filter bandwidth.

The basic equation of the Fabry–Perot etalon is given by

$$2\,\mu t\cos\theta = n\lambda \tag{2}$$

where μt is the optical spacing of the etalon and θ the angle of incidence. For integral values of n the constructive interference condition is satisfied and bright fringes are seen. For a camera lens of focal length F, the above equation (for small θ) simplifies to

$$2\mu t(1 - R^2/2F^2) = n\lambda \tag{3}$$

where R is the radius of a particular fringe. Using calibration interferogram μt is estimated. A grid of radii values for the first fringe is generated using the above spacer value for slightly different wavelength around Hα and the value for the best match with the observed radius is noted. The radius for the lower order (outer) fringes were then calculated with respect to the first fringe. From Equation (2) it follows that

$$R\mathrm{d}R/F^2 = \delta\lambda/\lambda = V/c$$

where $\mathrm{d}R = R_{\mathrm{cal}} - R_{\mathrm{obs}}$. Knowing the calculated and observed radii of the interference fringe pattern the relative velocity (V) of the observed Hα emission at various positions can be calculated.

Error Estimation

There are two sources of error: (i) The effective instrumental width of 0.11 Å results an error in velocity estimation to 5 km s^{-1}. (ii) The error due to sampling depends upon the radius at which the velocity is estimated and on the direction of the scan as defined by θ. This error is generally more than the error due to the instrumental limiting resolution. The errors are classified into two zones with high and low values and indicated appropriately in Fig. 3.

References

Alexander, C. J. Luhman, J. G., Russel, C. T. 1986, *Geophys. Res. Lett.*, **13,** 917.
Barnard, E. E. 1893, *Astr. Assoc. J.*, **9,** 59.

Bobrovnikoff, N. T. 1931, *Publ. Lick Obs.*, **17,** Part II, 309.
Brandt, J. C. 1968, *A. Rev. Astr. Astrophys.*, **6,** 267.
Brandt, J. E. 1982, in *Observations and Dynamics of Plasma Tail, Comets.*, Univ. Arizona Press, p. 519.
Burlaga, L. F., Rahe, J., Donn. B., Neugebauer, M. 1973, *Solar Phys.*, **30,** 211.
Chakaveh, S. C., Green, S. F., Ridley, J. H., McDonnell, J. A. M., Hughes, D. W. 1986, in *Proc. 20th ESLAB Symp. Exploration of Halley's Comet*, Heidelberg, ESA SP-250, Vol. 2, p. 163.
Chandrasekhar, T., Ashok, N. M., Debi Prasad, C., Desai, J. N. 1988, *Opt. Engg.*, **27,** 67.
Chandrasekhar, T., Debi Prasad, C., Desai, J. N., Ashok., N. M., Gupta, Ranjan 1987 in *Diversity and Similarity of Comets.*, ESA. SP-278, p. 567.
Cosmovici, C. B. 1987, *Astr. Astrophys.*, **63,** 83.
Cosmovici, C. B., Mack, P., Craubner, H., Schwarz, G. 1986, in *Proc. 20th ESLAB Symp. Exploration of Halley's Comet*, Heidelberg, ESA SP-250, Vol. 2, p. 151.
Cosmovici, C. B., Strafella, F., Dimagli, L., D'Innocenzo, A., Leggieri, G., Nesta, C., Perrone, A. 1978, *Astr. Astrophys.*, **63,** 83.
Delsemme, A. H. 1979 in *Space Missions to Comets*, NASA, 2089, p. 136.
de Pater, T., Palmer, P., Synder, L. E., Ip. W.-H. 1986, in *Proc. 20th ESLAB Symp. Exploration of Halley's Comet*, Heidelberg, ESA SP-250, Vol. 1, p. 409.
Donn, B., Urey, H. 1957, *Astrophys. J.*, **123,** 339.
Festou, M. C., Feldmann, P. D., A'Hearn, M. F., Arpigny, C., Cosmovici, C. B., Danks, A. C., McFadden, L. A., Gilmozzi, R., Patriarchi, P., Tozzi, G. P., Wallis, M. K., Weaver, H. A. 1986, *Nature*, **321,** 361.
Formisano, V., Amata, E., Agnelli, G., Bellucci, G., Cristaldi, S. 1986, in *Proc. 20th ESLAB Symp. Exploration of Halley's Comet*, Heidelberg, ESA SP-250, Vol. 3, p. 127.
Greenstein, J. L., 1962, *Astrophys. J.*, **136,** 686.
Grun. E., Graser, V., Kohoutek, L., Thick, U., Massonne, L., Schwehm, G. 1986, *Nature*, **321,** 144.
Ip. W.-H. 1980 *Astr. Astrophys.*, **92,** 95.
Ip. W.-H., Cosmovici, C. B., Mack, P. 1986, in *Proc. 20th ESLAB Symp. Exploration of Halley's Comet*, Heidelberg, ESA SP-250, Vol. 1, p. 207.
Jockers, K., 1985, *Astr. Astrophys. Suppl. Ser.*, **62,** 791.
Jockers, K., Geyer, E. H. 1985, *Messenger*, No. 42, 9.
Jockers, K., Lust, R. 1973, *Astr. Astrophys.*, 26, 113.
Kerr, R. B., Tepley, C. A., Cageao, R. P., Atreaya, S. K., Donahue, T. M., Cherchnneff, I. M. 1987, *Geophys. Res. Lett.*, **14,** 53.
Kresak, L. 1974, *Bull. Astr. Inst. Czech.* **25,** 293.
Lutz, B. L., Wagner, R. M. 1986, *Astrophys. J.*, **308,** 993.
McCoy, R. P., Opal, C. B., Carruthers, G. R. 1986, *Nature*, **324,** 439.
Neubauer, F. M., Glassmeier, K. H., Pohl, J., Raeder, J., Acuna, M. H., Burlaga, L. F., Ness, N. F., Musmann, G., Mariani, F., Wallis, M. K., Ungstrup, E., Schmidt, H. U. 1986, *Nature*, **321,** 352.
Niedner, M. B. 1980, *Astrophys. J.*, **24,** 820.
Niedner, M. B. 1986, *IHW Newsletter*, No. 9, 2.
Niedner, M. B., Brandt, J. C. 1978, *Astrophys. J.*, **223,** 655.
Niedner, M. B., Brandt, J. C. 1979, *Astrophys. J.*, **234,** 723.
Niedner, M. B., Brandt, J. C. 1980, *Icraus*, **92,** 257.
Niedner, M. B., Schwingenschuh, K. 1986, in *Proc. 20th ESLAB Symp. Exploration of Halley's Comet*, Heidelberg, ESA SP-250, Vol. 3, p. 419.
Roosen, R. G., Brandt, J. C. 1976, in *The Study of Comets*, Part I, NASA SP 393, p. 378.
Russell, C. T., Luhman, J. G. 1987, *Geophys. Res. Lett.*, **14,** 991.
Saito, T., Yumoto, K., Hirao, K., Nakagawa, T., Saito, K. 1986, *Nature*, **321,** 303.
Schleicher, D. G., Millis, R. L., Tholen, D., Lark, N., Birch, P. V., Martin, R., A'Hearn, M. F. 1986, in *Proc. 20th ESLAB Symp. Exploration of Halley's Comet*, Heidelberg, ESA SP-2501. Vol. 1, p. 565.
Somogyi, A. J. *et al.* 1986, *Nature*, **321,** 285.
Sulentic, J. W., Tifft, W. G. 1973, *The Revised New General Catalogue of Astronomical Objects*, Univ. Arizona Press.

Telesco, C. M., Decher, R., Baugher, C., Campins, H., Mozurkewich, D., Thronson, H. A., Cruikshank, D. P., Hammel, H. B., Larson, B., Sekanina, Z. 1986, *Astrophys. J.*, **310,** L61.
Vaisberg, O. L., Zastenker, G., Smirnov, V., Khazanov, B., Omelchenko, A., Fedorov, A., Zakharov, D. 1987, *Astr. Astrophys.*, **187,** 183.
Verigin, M. I., Axford, W. I., Gringauz, K. I., Richter, A. K. 1987, *Geophys. Res. Lett.*, **14,** 987.
Whipple, F. L. 1950, *Astrophys. J.*, **111,** 375.
Whipple, F. L. 1951, *Astrophys. J.*, **113,** 464.
Whipple, F. L. 1980, *Astr. J.*, **85,** 305.
Wolt, M. 1909, *Astr. Nacht.*, **180,** No. 4297, 1.
Wyckoff, S. 1982, in *Comets*, Ed. Wilkening, Univ. Arizona Press, p. 3.